Lytic immune synapse function requires filamentous actin deconstruction by Coronin 1A

Emily M. Mace and Jordan S. Orange[1]

Center for Human Immunobiology, Baylor College of Medicine and Texas Children's Hospital, Houston, TX 77030

Edited by Michael L. Dustin, Skirball Institute of Biomolecular Medicine, New York, NY, and accepted by the Editorial Board March 21, 2014 (received for review August 15, 2013)

Lytic immune effector function depends upon directed secretion of cytolytic granules at the immunological synapse (IS) and requires dynamic rearrangement of filamentous (F)-actin. Coronin 1A (Coro1A) is the hematopoietic-specific member of the Coronin family of actin regulators that promote F-actin disassembly. Here, we show that Coro1A is required for natural killer (NK) cell cytotoxic function in two human NK cell lines and ex vivo cells from a Coro1A-deficient patient. Using superresolution nanoscopy to probe the IS, we demonstrate that Coro1A promotes the deconstruction of F-actin density that facilitates effective delivery of lytic granules to the IS. Thus, we show, for the first time to our knowledge, a critical role for F-actin deconstruction in cytotoxic function and immunological secretion and identify Coro1A as its mediator.

cytotoxicity | superresolution microscopy | natural killer cells

Natural killer (NK) cell cytotoxicity is a finely controlled process that integrates signals from activating and inhibitory receptors to eliminate virally infected and tumorigenic cells sensitively and specifically. The importance for NK cells in immune function is underscored by the severe virus infections and malignancies suffered by patients with NK cell deficiency (1). A dynamic filamentous (F)-actin cytoskeleton is required for NK cell cytotoxicity because disruption of F-actin polymerization by pharmacological inhibitors or mutation of actin-nucleating factors results in impaired NK cell function (2–5). Actin nucleators, such as actin-related proteins 2 and 3 complex (Arp2/3), Wiskott–Aldrich syndrome protein (WASp), WIP, DOCK8, and WAVE2, serve well-defined critical roles in the formation and function of the NK cell immunological synapse (IS) (4–10).

Killing of a susceptible target follows tightly regulated steps of NK cell immune synapse formation and lytic granule exocytosis (3). Although cortical F-actin has long been considered a barrier to exocytosis of granule-like organelles (11) in some cell types, ligation of NK cell activating and adhesion receptors results in the formation of conduits in F-actin that permit and actually facilitate NK cell degranulation (12–14). This finding suggests that fine regulation and deconstruction of the synaptic F-actin meshwork is required for the formation of granule-permissive–sized clearances (12).

Coronin 1A (Coro1A) is the hematopoietic cell-specific isoform of the highly conserved Coronin family of actin regulators. Coronins contain a series of WD-repeat domains that form an F-actin–binding β-propeller domain, and thus bind F-actin directly (15–17). In addition, Coro1A binds to and inhibits the Arp2/3 complex (17, 18) required for actin branching and can enhance the activity of cofilin to promote actin disassembly in in vitro reconstituted systems (19–21). Coro1A localizes with actin-rich structures in immune cells, including phagocytic cups in neutrophils and macrophages, and at the leading edge of T cells (22–25). T cells from Coronin $1^{-/-}$ mice have defects in migration and cell survival attributed to impaired T-cell receptor signaling, Ca^{2+} flux, Rac activation, and subcellular Arp2/3 localization (26–28). Mutations in Coro1A lead to $T^{-}B^{+}NK^{+}$ combined immunodeficiency and susceptibility to severe viral infections, including life-threatening varicella infection and EBV-driven lymphoproliferation (26, 29, 30).

By manipulating expression of Coro1A in human NK cells, we show that Coro1A is required for cytotoxic function. Using superresolution nanoscopy, we define a requirement for Coro1A in F-actin deconstruction and subsequent delivery of lytic granules to the synaptic membrane. In addition, we have specifically evaluated cytotoxic function in a Coro1A-deficient patient and find that NK cell function is severely impaired. Further, we demonstrate the same F-actin structural defect in patient cells as in two Coro1A-deficient cell lines. Thus, with superresolution imaging, we identify, for the first time to our knowledge, a critical role for actin deconstruction in immunity and human host defense.

Results

Coro1A Localizes with F-Actin to the NK IS. Given the known ability of Coro1A to interact with F-actin, we initially determined its localization at the NK cell IS. YTS NK cells were incubated with susceptible 721.221 target cells and stained for Coro1A, F-actin, and perforin (as a marker of lytic granules). When visualized using confocal microscopy, Coro1A was found at the mature NK cell IS (Fig. 1*A*), which was defined by the accumulation of F-actin and the polarization of lytic granules. Quantitative analysis identified that 61.6 ± 19.2% of total cellular Coro1A was colocalized with F-actin. Ex vivo NK cells from human peripheral blood showed a similar pattern of Coro1A and actin localization, with 64.3 ± 10.4% of Coro1A associated with F-actin at the synapse (Fig. S1). To determine if the recruitment of Coro1A to the synapse occurs in concert with F-actin accumulation during synapse formation, we created a YTS NK cell line stably expressing Coro1A (CORO1A)-GFP and mCherry-actin. Using total internal reflection microscopy (TIRFm), we visualized live cells spreading on immobilized antibodies against activating receptors, which recapitulates the NK cell lytic IS (12, 31). Both

Significance

Natural killer (NK) cells are cytolytic effector cells of the innate immune system. They are critical for the control of viral infection and malignancy, and patients with impaired NK cell function have recurrent and often fatal viral infection and malignancy. NK cell cytotoxic function is exerted by secretion of specialized lytic granules. Here, we show that deconstruction of synaptic cortical filamentous (F)-actin by Coronin 1A (Coro1A) is required for NK cell cytotoxicity through the remodeling of F-actin to enable lytic granule secretion. We define this requirement for remodeling using superresolution nanoscopy and Coro1A-deficient NK cells. In addition, we use NK cells from a patient with a rare Coro1A mutation, thus illustrating a critical link between Coro1A function and human health.

Author contributions: E.M.M. and J.S.O. designed research; E.M.M. performed research; E.M.M. analyzed data; and E.M.M. and J.S.O. wrote the paper.

The authors declare no conflict of interest.

This article is a PNAS Direct Submission. M.L.D. is a guest editor invited by the Editorial Board.

[1]To whom correspondence should be addressed. E-mail: orange@bcm.edu.

This article contains supporting information online at www.pnas.org/lookup/suppl/doi:10.1073/pnas.1314975111/-/DCSupplemental.

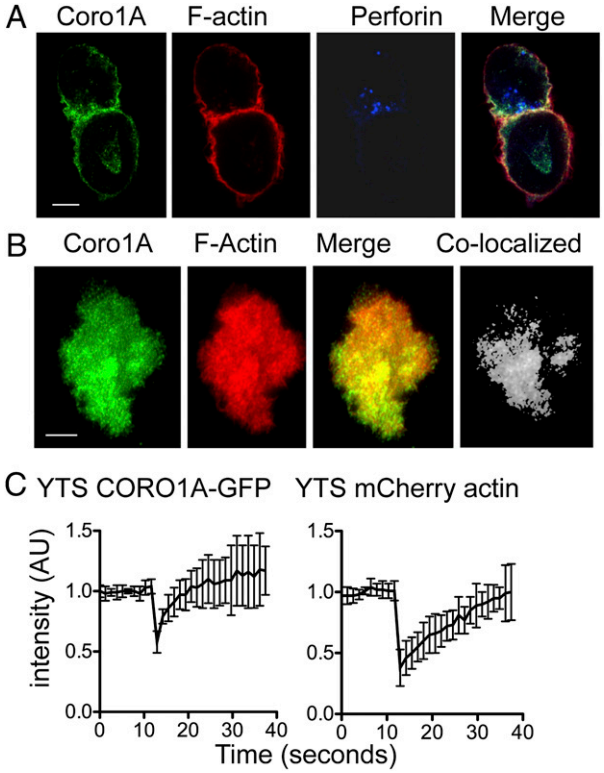

Fig. 1. Coro1A localizes to the NK cell cytolytic IS. (*A*) YTS NK cells conjugated to 721.221 target cells were fixed, permeabilized, and stained for Coro1A (green, *Far Left*), F-actin with phalloidin (red, *Left Center*), and perforin (blue, *Right Center*). (*B*) YTS-CORO1A-GFP mCherry-actin cells activated by immobilized antibody on glass were imaged at one frame per minute by TIRFm. Shown are representative images 10 min after contact with the imaging chamber. (*Far Right*) Colocalized pixels were calculated and are shown in grayscale. (*C*) YTS-CORO1A-GFP mCherry-actin cells were activated with immobilized antibody for 10 min, and fluorescence was bleached to 50% for both GFP and mCherry fluorophores. Fluorescent intensity for both channels was normalized, and the mean ± SD is shown for eight cells from three independent experiments. AU, arbitrary units. (Scale bars: 5 μm.)

Coro1A and actin were present in the cell cortex as NK cells spread, and after 10 min, there was substantive colocalization between Coro1A and F-actin (63.9 ± 12.7%; Fig. 1*B*).

To determine if Coro1A was dynamically recruited to the IS akin to F-actin, we measured fluorescence recovery after photobleaching (FRAP) of CORO1A-GFP and mCherry-actin at the NK cell synapse following activation. After simultaneous photobleaching, both molecules quickly recovered to the depleted area (Fig. 1*C*). Interestingly, Coro1A appeared to be recruited more quickly ($\tau_{1/2}$ = 1.4 ± 0.7 s) than actin ($\tau_{1/2}$ = 7.8 ± 4.7 s) in all cells evaluated (n = 7; Movie S1). To ensure that the quicker recovery of Coro1A was not a function of the GFP molecule, we bleached YTS GFP-actin cells using the same conditions and found that GFP-actin and mCherry-actin recovery dynamics were similar (Fig. S2). Thus, Coro1A is recruited to the lytic NK IS during the stage of F-actin accumulation and colocalizes with actin through the duration of the mature synapse.

Coro1A Is Required for NK Cell Lytic Function. To evaluate the role of Coro1A in NK cell cytotoxicity, we stably expressed Coro1A-shRNA in YTS NK cells. shRNA expression nearly completely abrogated Coro1A protein expression (Fig. S3*A*). Because loss of Coro1A has been reported previously to increase basal levels of F-actin (22, 24, 26), we measured the ratio of monomeric (G)-actin to F-actin found in these cell lines by comparing soluble and insoluble cell fractions (Fig. 2*A*). The loss of Coro1A did not affect the distribution of actin, and thus did not simply result in redistribution of actin forms.

To determine the utility of Coro1A in NK cell cytotoxicity, lytic activity was evaluated by ^{51}Cr-release assays. Loss of Coro1A significantly decreased NK cell cytotoxic function in standard 4-h assays (Fig. 2*B*, *Right*). To determine if this loss of function was owing to an inability to mediate an initial kill or to decreased efficiency of subsequent kills, we evaluated cytotoxic activity after only 1 h. Here, the defect in Coro1A-deficient cells was near absolute, suggesting the former (Fig. 2*B*, *Left*). To probe the mechanism underlying this functional defect in Coro1A-deficient cells, we performed fluorescence-activated cell sorting–based degranulation assays. Despite forming effective and even increased conjugates with target cells (Fig. 2*C*), YTS-CORO1A knockdown (KD) cells had decreased degranulation as measured by cell surface CD107a expression at both 1 and 2 h (Fig. 2*D*). This defect could have been a feature of ineffective activation signaling after cell conjugation and activation receptor ligation, because Coro1A has been reported to be required for Rac activation and recruitment (28). Thus, we performed immunoblotting for phosphorylated ERK in cells activated on immobilized antiactivating receptor antibody. ERK phosphorylation, which is a downstream indicator of Rac activation, was comparable between Coro1A-sufficient and Coro1A-deficient cell lines (Fig. 2*E*), thus demonstrating that activation receptor signaling in NK cells was independent of Coro1A. To test downstream activation in Coro1A-deficient cells further, we measured intracellular calcium concentration following activation and found it to be robust [2.4 ± 0.04-fold increase in YTS-CORO1A-KD vs. 2.3 ± 0.27-fold increase in YTS empty vector (EV)] (Fig. S3*B*). Similarly, STAT5 phosphorylation following IL-2 stimulation was comparable to that of controls (6.5 ± 0.64-fold increase in YTS-CORO1A-KD vs. 5 ± 0.37-fold increase in YTS-EV) (Fig. S3*C*). Finally, we tested IFN-γ secretion following overnight incubation with susceptible target cells. Both YTS-EV and YTS-CORO1A-KD cells showed significant and comparable

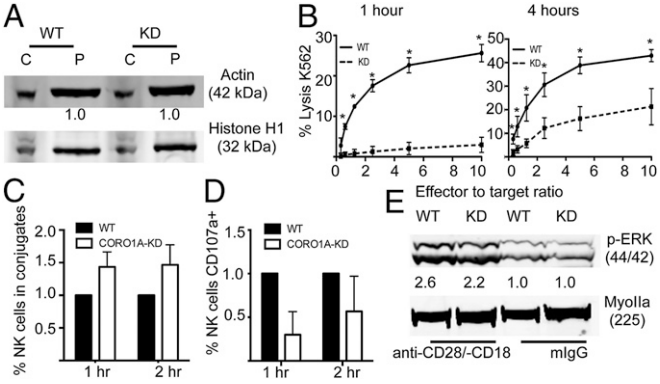

Fig. 2. Coro1A is required for NK cell cytotoxic function but not activation. YTS cells were stably transfected with CORO1A-KD shRNA or EV. (*A*) YTS-EV or YTS-CORO1A-KD cells were lysed and fractionated by high-speed centrifugation; cytoplasmic (C) and insoluble pellet (P) fractions were then immunoblotted for actin and Histone H1 as a loading control. (*B*) YTS-EV (solid line) or YTS-CORO1A-KD (dashed line) cells were incubated with susceptible 721.221 target cells for 1 h (*Left*) or 4 h (*Right*), and cell lysis was assayed by standard ^{51}Cr-release assay. The mean ± SD of four independent experiments is shown. *P < 0.05 by Student's two-tailed unpaired t test. (*C* and *D*) Conjugates were formed as described in *Materials and Methods* in the presence of anti-CD107a to assess NK cell degranulation. YTS-EV (black) cells were normalized to 1. (*E*) YTS-EV (WT) or YTS-CORO1A-KD (KD) cells were activated for 10 min on anti-CD18 and anti-CD28 or mouse IgG as a negative control. Cells were immunoblotted for phosphorylated ERK or Myosin IIA as a loading control. Shown is one representative blot from three independent experiments.

IFN-γ secretion as measured by ELISA (Fig. S3*D*). With conjugate formation and activation signaling intact in YTS-CORO1A-KD cells, we hypothesized that the role for Coro1A in NK cell cytotoxicity was through enabling lytic synapse function required for target cell killing.

Coro1A Loss Results in Increased F-Actin Density at the NK IS. We next evaluated the effect of Coro1A disruption on IS formation and lytic granule polarization to determine where in the stepwise process an abnormality might lie. Using confocal microscopy, we found signs of a mature lytic synapse with F-actin accumulated at and lytic granules polarized to the synapse after target cell conjugation (Fig. 3*A*). Quantification of F-actin accumulation showed no increase in the total amount present at the synapse in Coro1A-deficient cells (117.9 ± 22.4 vs. 100.5 ± 21.0 arbitrary units) (Fig. S4*A*). Measurement of granule polarization (distance of the granule region centroid to the IS) and centrosome polarization was also not significantly affected by the loss of Coro1A (Fig. S4 *B* and *C*). YTS-CORO1A-KD cells showed no difference in the size of the IS formed with target cells (Fig. S4*D*) or in the accumulation of CD11a (LFA-1) at the synapse, which is an actin-dependent process (32) (Fig. S4*E*). Thus, the assembly of the synapse and relatively late steps in lytic synapse maturation required for cytotoxicity (granule polarization) were intact in the absence of Coro1A.

To determine if a slight change in synaptic actin could be an indication of a relevant alteration, we probed the actin architecture more closely using stimulated emission depletion (STED) imaging. Superresolution nanoscopy was performed at the plane of the synapse in cells that had been activated by immobilized antibody and stained with phalloidin. Coro1A-deficient cells had a greater density, yet decreased area, of F-actin (Fig. 3*B* and Fig. S4*F*), which was confirmed in quantitative analyses of >100 cells (Fig. 3 *C* and *D*). Examination of Coro1A localization at the synapse showed a high degree of colocalization with F-actin and a lesser degree of colocalization with Arp2/3 (Fig. S5 *A*–*C*). Synaptic recruitment of Arp2/3 was not prevented by Coro1A deficiency (Fig. S5 *D* and *E*).

With increased density of synaptic F-actin, it was possible that degranulation is obstructed in the absence of Coro1A, because lytic granules are secreted through hypodense regions of the F-actin network at the NK cell synapse (12–14). To determine if Coro1A is required for the formation of granule-permissive openings in actin meshworks, we measured activation-induced clearances in the synaptic F-actin network using STED imaging. When these clearances were evaluated considering size, Coro1A-deficient cells had a prominent and significant decrease in 250- to 500-nm clearances (Fig. 3*E*). To confirm these findings, we created a second Coro1A-deficient cell line using NK92 NK cells. Similar to YTS NK cells, loss of Coro1A in NK92 cells resulted in an increase in F-actin mean fluorescent intensity (MFI) at the synapse and a decrease in granule-permissive–sized clearances, accompanied by a defect in NK92 cytotoxic function (Fig. S6). Overall, these observations suggest that Coro1A is required for fine control of F-actin density at the NK IS, and resultant conduit formation required for granule penetrance so that the granules might reach the synaptic membrane, but that it is not required for normal IS formation.

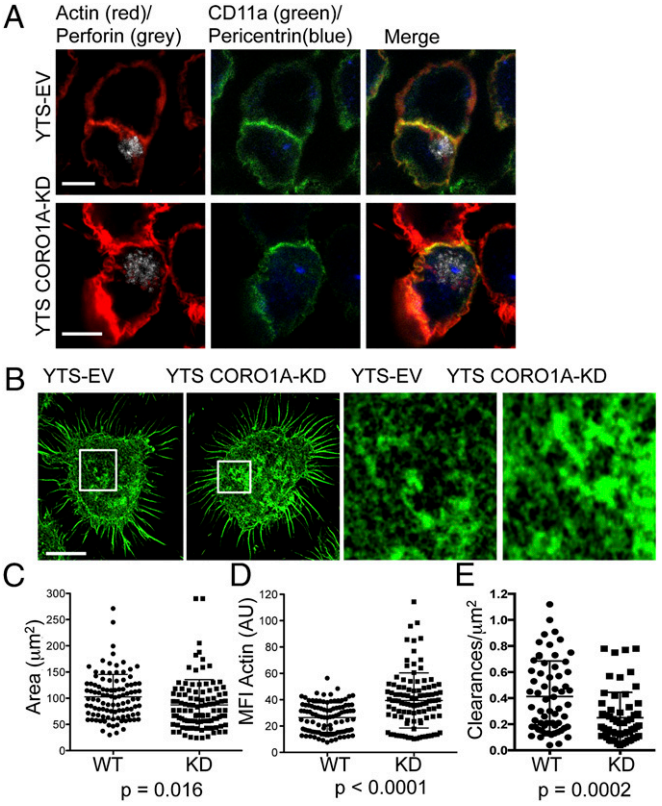

Fig. 3. Superresolution imaging defines a requirement for Coro1A in the control of F-actin density at the NK synapse. (*A*) YTS-EV or YTS-CORO1A-KD cells were incubated with susceptible 721.221 target cells and then fixed, permeabilized, and stained for CD11a (green), F-actin with phalloidin (red), perforin (gray), and pericentrin (blue). (*B*) YTS-EV or YTS-CORO1A-KD cells were incubated on immobilized activating antibody and then fixed, permeabilized, and stained for F-actin and imaged at the plane of glass by STED nanoscopy. (*Right*) Detailed structure of F-actin is shown for the highlighted regions. Shown are representative images from four independent experiments. (Resolution: 60 nm.) The area (*C*; square micrometers) and MFI (*D*) of F-actin staining were measured for YTS-EV (●) and YTS-CORO1A-KD (■) cells (all excluding cell cortex). Shown are 104 cells from four independent experiments, with one data point representing each cell. (*E*) F-actin clearances per square micrometer permissive for lytic granule secretion (250–500 nm) were measured for YTS-EV (●) and YTS-CORO1A-KD (■) cells. Each data point represents clearances per square micrometer for one cell. Shown are 60 cells from three independent experiments. (Scale bars: 5 μm.)

Coro1A Is Required for Lytic Granule Penetration of the F-Actin Cortex. Given the requirement for Coro1A in generating the full repertoire of potential access points for lytic granules in synaptic F-actin, we evaluated the subdiffraction-limited relationship between granules and F-actin using dual-channel STED nanoscopy to determine if there might be inappropriate approximation between cortical actin and the granules. Coro1A-deficient cells had a significantly greater amount of F-actin associated with lytic granules at the lytic synapse (Fig. 4*A*, *Left*). Although granules in Coro1A-sufficient cells were observed to sit in hypodensities of F-actin (Fig. 4*A*, *Right*), those in Coro1A-deficient cells were associated with increased F-actin intensity (measured by dual-channel profiles of actin and perforin; Fig. 4*B*). These observations were further borne out quantitatively across multiple granules and cells as there was a greater than twofold increase in F-actin associated with perforin in Coro1A-deficient cells and an increased intensity of F-actin at granules (Fig. 4 *C* and *D*). Thus, there was a decreased probability for NK cell lytic granules to reside in F-actin hypodensities in the absence of Coro1A.

We next asked if the increased F-actin density and association with granules, in concert with fewer granule-permissive–sized clearances, affected the ability of granules to traverse the F-actin network at the cortex to approach the synaptic membrane. These experiments were performed using TIRFm in living NK cells loaded with LysoTracker Red dye to allow for selective visualization of lytic granules within ∼150 nm of the synaptic membrane. Coro1A deficiency resulted in an almost twofold reduction in the number of lytic granules found in the NK cell cortex (Fig. 4 *E* and *F*). The fewer number of granules that were present at the cortex of Coro1A-deficient cells, however, demonstrated normal

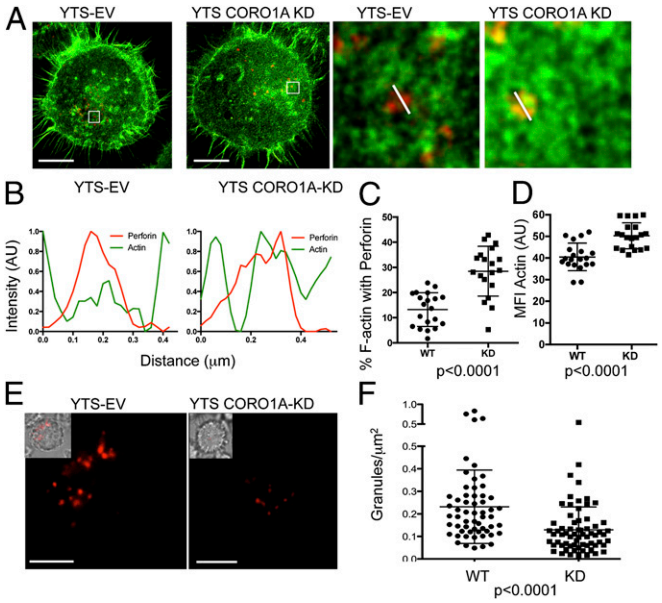

Fig. 4. Coro1A is required for actin disassembly to facilitate granule penetrance at the IS. (*A*) YTS-EV and YTS-CORO1A-KD cells activated with immobilized activating antibody were stained for F-actin and perforin, and then imaged at the plane of glass by dual-channel STED nanoscopy. (Scale bars: 5 μm.) (Resolution: F-actin, 50 nm; perforin, 60 nm.) (*Right*) Detailed images from highlighted boxes are shown. (*B*) Line profiles drawn across the granules shown in *A* are shown for YTS-EV (*Left*) and YTS-CORO1A-KD (*Right*). Fluorescence intensity of F-actin staining is shown as a green line, and perforin fluorescence intensity is shown in red. (*C*) Percentage of F-actin colocalized with perforin (excluding cell cortex) was calculated for YTS-EV (●) and YTS-CORO1A-KD (■) cells imaged by STED nanoscopy as in *A*. (*D*) Lytic granules were identified, and MFI of actin was measured for YTS-EV (●) and YTS-CORO1A-KD (■) cells. Each symbol represents the mean of all granules from one cell ($n = 20$ from two independent experiments). (*E*) YTS-EV and YTS-CORO1A-KD cells were loaded with Lysotracker Red and imaged by TIRFm after 10 min of incubation in an imaging chamber coated with immobilized activating antibody. (Scale bars: 5 μm.) (*Inset*) Differential interference contrast merged images are shown. (*F*) Granules per square micrometer found in the membrane proximal TIRFm field are shown for YTS-EV (●) and YTS-CORO1A-KD (■) cells. Each data point represents one cell ($n = 50$ from three independent experiments).

kinetics and degranulated with the same frequency as WT cells (Fig. S7 and Movie S2). Thus, Coro1A is not required for granule movement but specifically facilitates granule penetrance through F-actin by promoting cortical actin hypodensities. Interestingly, stabilization of F-actin with Jasplakinolide specifically after formation of the IS also results in a decrease in the number of granule-permissive clearances, an increase in F-actin MFI, and a reduced F-actin area, and thus is consistent with the state of synaptic F-actin in Coro1A deficiency (Fig. S8). However, despite differences in the F-actin area between control and Coro1A deficient cells, Coro1A-deficient cells showed normal cell spreading when measured by differential interference contrast microscopy, thus suggesting a role for Coro1A specifically in F-actin nanorestructuring (Fig. S9).

Three-Dimensional STED Nanoscopy of F-Actin Demonstrates a Requirement for Coro1A in F-Actin Meshwork Structure and Synaptic Lytic Granule Approximation. Because our 2D data suggested that Coro1A was essential in reducing the potential for F-actin to serve as a barrier to degranulation, we evaluated F-actin after NK cell activation in three dimensions by STED specifically to define the potential for barrier structure (Fig. 5*A*). Although 3D surface rendering supported the observations made in two dimensions of increased F-actin density in Coro1A-deficient cells, 3D reconstruction demonstrated volumetric synaptic differences (Movie S3). Coro1A deficiency resulted in decreased F-actin volume but increased F-actin intensity (Fig. 5*B*). Thus, in the absence of Coro1A, the F-actin meshwork at the synaptic membrane was a denser and more confined barrier, and thus less penetrable.

The observation that Coro1A-deficient cells had less volume and greater F-actin density was also supported by evaluation of *x*,*z*-axis reconstructions (Fig. 5*C*). These reconstructions demonstrated that the increased intensity of F-actin caused by Coro1A deficiency was not due to increased actin volume in the *z*-axis plane, and thus represented a more compact synaptic membrane-proximal barrier. This observation was quantified using 20 radial intensity plots of surface-rendered 3D reconstructions, which showed overall increased F-actin intensity in Coro1A-deficient cells ($P < 0.0001$, Mann–Whitney *U* test) (Fig. 5*D*). Finally, we reconstructed images of the lytic synapse to include F-actin and perforin using STED. Coro1A-deficient cells had increased intensity of F-actin staining as seen previously. Importantly, the lytic granules were positioned on top of a noticeably dense F-actin cortex in the Coro1A-deficient cells. This positioning was in contrast to the Coro1A-sufficient cells, where granules had penetrated the cortex and resided at the synaptic membrane (Fig. 5*E*). Thus, using superresolution nanoscopy, we resolved the effect of Coro1A deficiency upon F-actin and granule dynamics. Specifically, Coro1A was required for fine reorganization, and thus deconstruction, of the cortical F-actin meshwork to create hypodense regions allowing lytic granules to approximate the synaptic membrane.

Naturally Occurring Human Coro1A Deficiency Results in Impaired NK Cell Cytotoxic Function and Increased F-Actin Density at the IS. To determine the effect of Coro1A on immune function and ex vivo NK cells, we evaluated a new patient with a compound heterozygous *CORO1A* mutation: a c.1077delC (maternal source) in combination with a previously described c.248_249delCT (paternal source). Clinically, the patient presented with chronic human papilloma virus-epidermodysplasia verruciformis and severe oral herpetic lesions. Profound T-cell lymphopenia was detected;

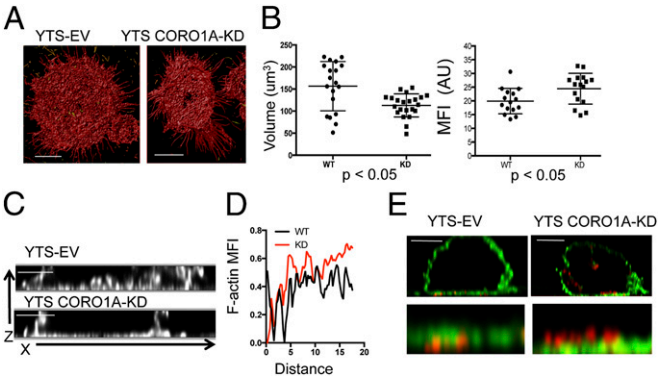

Fig. 5. Increased density of F-actin in the absence of Coro1A is defined by 3D STED. YTS-EV and YTS-CORO1A-KD cells were immobilized on glass coated with antibody to activating receptor and then fixed, permeabilized, and stained for F-actin. Cells were imaged by time-gated STED in 200-nm slices of the membrane-proximal 2 μm of cells. (*A*) Images were deconvolved and reconstructed in three dimensions and then surface-rendered. (Scale bars: 5 μm.) (Resolution: *z* axis, 200 nm.) (*B*) Volume and MFI of F-actin were measured for YTS-EV (●) and YTS-CORO1A-KD (■) cells. Each data point represents one of 20 cells from three independent experiments. (*C*) Cells were activated and stained as in *A*. Shown are representative images in the *X*,*Z* plane from YTS-EV and YTS-CORO1A-KD cells. (Scale bars: 2 μm.) (*D*) Radial intensity profiles of images generated as in *C* were normalized and plotted for 20 cells. (*E*) Cells were prepared as in Fig. 4 and imaged in 3D, time-gated STED for F-actin (green) and perforin (red). Shown are representative images from three experiments. (Scale bars: 5 μm.)

however, patient NK cells were present as normal percentages of peripheral blood lymphocytes but had severely impaired cytotoxic function against K562 erythroblast target cells compared with a normal control (Fig. 6*A*). To determine if the effect on F-actin architecture seen in the Coro1A-deficient cell line could be identified in patient cells, we performed STED nanoscopy as in Fig. 3. NK cells from the patient and a normal donor were activated on anti-CD18 and anti-NKp30, and were then stained with phalloidin and antiperforin antibody, and imaged by STED (Fig. 6*B*). Comparable to the Coro1A-KD cell line, patient cells had a uniformly smaller area of F-actin than NK cells from a normal donor (42.1 ± 29.6 μm vs. 75.6 ± 26.4 μm) (Fig. 6*C*). This decrease in area was accompanied by a significant increase in intensity of F-actin staining (Fig. 6*D*). To determine if this increase in F-actin intensity was acting as a barrier to lytic granule release, the frequency of clearances in F-actin permissive for lytic granule secretion were measured in patient and normal donor cells. Patient cells had significantly fewer clearances permissive for lytic granules (Fig. 6*E*). Therefore, an NK cell functional defect in a Coro1A-deficient patient relates to altered F-actin architecture as demonstrated by STED nanoscopy. The fine control of F-actin meshwork in human NK cells needed for lytic granule access to the synaptic membrane is an essential Coro1A-dependent regulatory step in accessing cytotoxic defense.

Discussion

F-actin at the NK IS is found in a pervasive yet permissive network. Ligation of NK cell-activating receptors results in the formation of clearances in the cortical F-actin to enable lytic granule secretion. These clearances range in size, as do lytic granules themselves (12). Here, we show that Coro1A is required for effective granule secretion through the deconstruction of F-actin at the IS, specifically for the generation of a sufficient number of granule-permissive–sized clearances. Loss of these clearances in the absence of Coro1A is accompanied by a decrease in efficiency of NK cell cytotoxicity. This work identifies, for the first time to our knowledge, an actin disassembly factor as a critical regulator of not only cytolytic function but also immune cell secretion. In addition, we show a role for this actin disassembly in human health, because NK cells from a patient with biallelic Coro1A mutations have functional NK cell deficiency, which we show is accompanied by altered F-actin architecture as seen in the cell line. Because the patient suffered from a characteristic susceptibility to NK cell defense-dependent pathogens, actin disassembly is likely to represent a relevant feature of human host defense.

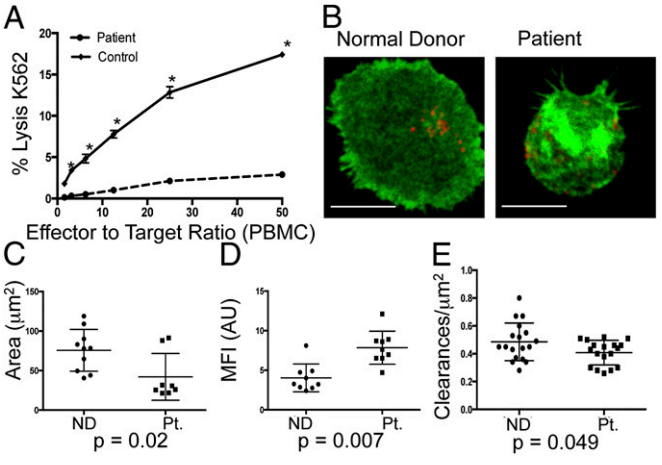

Fig. 6. NK cells from a Coro1A-deficient patient have defective cytotoxic function and altered F-actin architecture. (*A*) Peripheral blood mononuclear cells (PBMCs) from the patient (dashed line) or a healthy donor control (solid) were incubated with susceptible K562 targets, and specific lysis of targets was measured by standard ^{51}Cr-release assay. *$P < 0.05$ by Student's two-tailed unpaired *t* test. (*B*) NK cells from a normal donor (*Left*) or the patient (*Right*) were enriched by negative selection and analyzed by STED nanoscopy at the plane of the glass as in Fig. 3. Shown is one representative cell from two independent experiments. (Scale bars: 5 μm.) (Resolution: 110 nm.) Area (*C*, square micrometers) and MFI (*D*) of F-actin were measured as in Fig. 3 ($n = 10$ from three independent experiments). (*E*) F-actin clearances per square micrometer (250–500 nm) were measured for cells from the normal donor (●) and the patient (■). Each data point represents clearances per square micrometer for one cell ($n = 18$ cells per condition). ND, normal donor; Pt., patient.

Coronin $1^{-/-}$ mice have a particular defect in T-cell homeostasis, specifically in homing and migration of terminally mature peripheral αβ T cells (22, 27). Analysis of these mice and Coro1A-deficient human patients also shows a role for Coro1A in the localization of Arp2/3 within the cell and the regulation of its function (26, 27). Importantly, in Coro1A-deficent NK cells, we did not observe any alteration in Arp2/3 localization to the IS, and although Coro1A colocalizes highly with F-actin at the synapse, it is found less frequently with Arp2/3. Although it does not appear to be required for the localization of Arp2/3, Coro1A may be binding Arp2/3 to promote the turnover of F-actin, as has been proposed biochemically for Coronin 1 (16). Collectively, these results suggest a complexity in the role of Coro1A, as well as its participation in signaling, actin dynamics, motility, and homeostasis.

All previously described Coro1A-deficient patients have seemingly unaffected NK cell numbers; however, NK cells have not been studied functionally before now (26, 29, 30). It is relevant that these patients have recurrent and severe viral infections, and one of these patients was hospitalized with near-fatal varicella infection (26). Because recurrent and severe varicella infection is a hallmark of NK cell deficiency (1), one could speculate that NK cell function may also have been affected by Coro1A mutation. Our findings with NK cells do not preclude a T-cell defect in the patient that contributes to the clinical phenotype. However, our finding of specific NK cell functional deficiency and the correlation of F-actin architectural defects shows that NK cells, although not developmentally affected, have compromised effector function.

Importantly, our study uses high- and superresolution imaging to highlight the importance of the control and deconstruction of F-actin architecture in NK cell function. Although previous studies have shown an increase in the global level of F-actin in Coronin 1-deficient immune cells (22, 26, 27), we did not detect such a difference in the cell line or in patient cells. In addition, global levels of Rac activation and Ca^{++} flux were not affected, suggesting the downstream activation signaling required for cytotoxicity was intact in our Coro1A-deficient NK cells. Similarly, IFN-γ and STAT5 phosphorylation were intact in Coro1A-deficient NK cells, suggesting global activation was not impaired. When imaged by conventional confocal microscopy, however, Coro1A-deficient cells had no detectable increase in F-actin depth at the synapse. Through the first use, to our knowledge, of timegated STED microscopy in the immune system with unprecedented 3D resolution, we show an increase in F-actin density that does not correlate with an increase in F-actin depth. This increased density, in turn, dictates decreases in minimally sized granule-permissive clearances that are needed for lytic granule secretion.

Although it may seem surprising that a seemingly small effect on F-actin architecture translates to such a significant functional defect, our findings define the importance of the subtle control of F-actin clearance at the synapse. We propose that localized regulation of synaptic F-actin meshwork density controls secretory function to avoid inappropriate degranulation. This model is supported by the recent observation that localized oscillations in Ca^{2+}, PtdIns(4,5)P2, and N-WASP drive transient increases in cortical F-actin polymerization that allow for maximal efficiency of mast cell receptor-triggered granule secretion in rat basophilic leukemia cells (33). It is reasonable to hypothesize that activating signal in NK cells also results in localized actin dynamics and that

this localized control of F-actin deconstruction is as critical as its polymerization. With the enhanced resolution offered by advanced superresolution imaging technology, we demonstrate here that F-actin deconstruction is required for the access of large lytic granules to the synaptic membrane to enable cytotoxic function.

Materials and Methods

Cell Lines, ex Vivo NK Cells, and Transfection. Generation of cell lines is described in detail in *SI Materials and Methods*. All human samples were obtained with written consent in accordance with Institutional Review Board approval at Texas Children's Hospital. Genetic details of the Coro1A-deficient patient will be described elsewhere, but c.1077delC (maternal source) and c.248_249delCT (paternal source) mutations were identified in the patient initially via whole-exome sequencing and were subsequently confirmed using the Sanger method. The c.248_249delCT mutation has been previously reported (29).

^{51}Cr-Release Cytotoxicity Assay. Standard ^{51}Cr-release assays were performed to test NK cell cytolytic activity against 721.221 target cells as described previously (34).

Western Blot Analysis and Cytoskeletal Fractionation Assay. Western blots were performed as described previously (5) and are described in detail in *SI Materials and Methods*.

Fluorescence-Activated Cell Sorting–Based Assays. Flow cytometric analysis of conjugate formation, degranulation, intracellular calcium concentration, and STAT5 phosphorylation is described in detail in *SI Materials and Methods*.

Confocal, STED, and TIRFm. NK cell conjugation to targets was performed as previously described (32, 35). Confocal, STED, and TIRFm and analysis are described in detail in *SI Materials and Methods*.

FRAP. FRAP was performed as described in *SI Materials and Methods*. Data were normalized using easyFRAP software (36).

ACKNOWLEDGMENTS. We thank Dr. L. Noroski for coordinating the Coro1A patient sample. We also thank the patient and patient's family for their contribution to this research. This work was supported by National Institutes of Health Grant R01067946 (to J.S.O.).

1. Orange JS (2006) Human natural killer cell deficiencies. *Curr Opin Allergy Clin Immunol* 6(6):399–409.
2. Katz P, Zaytoun AM, Lee JH, Jr. (1982) Mechanisms of human cell-mediated cytotoxicity. III. Dependence of natural killing on microtubule and microfilament integrity. *J Immunol* 129(6):2816–2825.
3. Wulfing C, Purtic B, Klem J, Schatzle JD (2003) Stepwise cytoskeletal polarization as a series of checkpoints in innate but not adaptive cytolytic killing. *Proc Natl Acad Sci USA* 100(13):7767–7772.
4. Butler B, Cooper JA (2009) Distinct roles for the actin nucleators Arp2/3 and hDia1 during NK-mediated cytotoxicity. *Curr Biol* 19(22):1886–1896.
5. Orange JS, et al. (2011) IL-2 induces a WAVE2-dependent pathway for actin reorganization that enables WASp-independent human NK cell function. *J Clin Invest* 121(4):1535–1548.
6. Krzewski K, Chen X, Orange JS, Strominger JL (2006) Formation of a WIP-, WASp-, actin-, and myosin IIA-containing multiprotein complex in activated NK cells and its alteration by KIR inhibitory signaling. *J Cell Biol* 173(1):121–132.
7. Krzewski K, Chen X, Strominger JL (2008) WIP is essential for lytic granule polarization and NK cell cytotoxicity. *Proc Natl Acad Sci USA* 105(7):2568–2573.
8. Lanzi G, et al. (2012) A novel primary human immunodeficiency due to deficiency in the WASP-interacting protein WIP. *J Exp Med* 209(1):29–34.
9. Ham H, et al. (2013) Dedicator of cytokinesis 8 interacts with talin and Wiskott-Aldrich syndrome protein to regulate NK cell cytotoxicity. *J Immunol* 190(7):3661–3669.
10. Orange JS (2008) Formation and function of the lytic NK-cell immunological synapse. *Nat Rev Immunol* 8(9):713–725.
11. Aunis D, Bader MF (1988) The cytoskeleton as a barrier to exocytosis in secretory cells. *J Exp Biol* 139:253–266.
12. Rak GD, Mace EM, Banerjee PP, Svitkina T, Orange JS (2011) Natural killer cell lytic granule secretion occurs through a pervasive actin network at the immune synapse. *PLoS Biol* 9(9):e1001151.
13. Brown AC, Dobbie IM, Alakoskela JM, Davis I, Davis DM (2012) Super-resolution imaging of remodeled synaptic actin reveals different synergies between NK cell receptors and integrins. *Blood* 120(18):3729–3740.
14. Brown AC, et al. (2011) Remodelling of cortical actin where lytic granules dock at natural killer cell immune synapses revealed by super-resolution microscopy. *PLoS Biol* 9(9):e1001152.
15. de Hostos EL (1999) The coronin family of actin-associated proteins. *Trends Cell Biol* 9(9):345–350.
16. Gandhi M, Goode BL (2008) Coronin: The double-edged sword of actin dynamics. *Subcell Biochem* 48:72–87.
17. Machesky LM, et al. (1997) Mammalian actin-related protein 2/3 complex localizes to regions of lamellipodial protrusion and is composed of evolutionarily conserved proteins. *Biochem J* 328(Pt 1):105–112.
18. Humphries CL, et al. (2002) Direct regulation of Arp2/3 complex activity and function by the actin binding protein coronin. *J Cell Biol* 159(6):993–1004.
19. Brieher WM, Kueh HY, Ballif BA, Mitchison TJ (2006) Rapid actin monomer-insensitive depolymerization of Listeria actin comet tails by cofilin, coronin, and Aip1. *J Cell Biol* 175(2):315–324.
20. Kueh HY, Charras GT, Mitchison TJ, Brieher WM (2008) Actin disassembly by cofilin, coronin, and Aip1 occurs in bursts and is inhibited by barbed-end cappers. *J Cell Biol* 182(2):341–353.
21. Ono S (2003) Regulation of actin filament dynamics by actin depolymerizing factor/cofilin and actin-interacting protein 1: New blades for twisted filaments. *Biochemistry* 42(46):13363–13370.
22. Föger N, Rangell L, Danilenko DM, Chan AC (2006) Requirement for coronin 1 in T lymphocyte trafficking and cellular homeostasis. *Science* 313(5788):839–842.
23. Grogan A, et al. (1997) Cytosolic phox proteins interact with and regulate the assembly of coronin in neutrophils. *J Cell Sci* 110(Pt 24):3071–3081.
24. Nal B, et al. (2004) Coronin-1 expression in T lymphocytes: Insights into protein function during T cell development and activation. *Int Immunol* 16(2):231–240.
25. Ferrari G, Langen H, Naito M, Pieters J (1999) A coat protein on phagosomes involved in the intracellular survival of mycobacteria. *Cell* 97(4):435–447.
26. Shiow LR, et al. (2008) The actin regulator coronin 1A is mutant in a thymic egress-deficient mouse strain and in a patient with severe combined immunodeficiency. *Nat Immunol* 9(11):1307–1315.
27. Mugnier B, et al. (2008) Coronin-1A links cytoskeleton dynamics to TCR alpha beta-induced cell signaling. *PLoS ONE* 3(10):e3467.
28. Castro-Castro A, et al. (2011) Coronin 1A promotes a cytoskeletal-based feedback loop that facilitates Rac1 translocation and activation. *EMBO J* 30(19):3913–3927.
29. Shiow LR, et al. (2009) Severe combined immunodeficiency (SCID) and attention deficit hyperactivity disorder (ADHD) associated with a Coronin-1A mutation and a chromosome 16p11.2 deletion. *Clin Immunol* 131(1):24–30.
30. Moshous D, et al. (2013) Whole-exome sequencing identifies Coronin-1A deficiency in 3 siblings with immunodeficiency and EBV-associated B-cell lymphoproliferation. *J Allergy Clin Immunol* 131(6):1594–1603.
31. Bryceson YT, March ME, Barber DF, Ljunggren HG, Long EO (2005) Cytolytic granule polarization and degranulation controlled by different receptors in resting NK cells. *J Exp Med* 202(7):1001–1012.
32. Orange JS, et al. (2003) The mature activating natural killer cell immunologic synapse is formed in distinct stages. *Proc Natl Acad Sci USA* 100(24):14151–14156.
33. Wollman R, Meyer T (2012) Coordinated oscillations in cortical actin and Ca2+ correlate with cycles of vesicle secretion. *Nat Cell Biol* 14(12):1261–1269.
34. Orange JS, et al. (2002) Wiskott-Aldrich syndrome protein is required for NK cell cytotoxicity and colocalizes with actin to NK cell-activating immunologic synapses. *Proc Natl Acad Sci USA* 99(17):11351–11356.
35. Banerjee PP, et al. (2007) Cdc42-interacting protein-4 functionally links actin and microtubule networks at the cytolytic NK cell immunological synapse. *J Exp Med* 204(10):2305–2320.
36. Rapsomaniki MA, et al. (2012) easyFRAP: An interactive, easy-to-use tool for qualitative and quantitative analysis of FRAP data. *Bioinformatics* 28(13):1800–1801.